

Patient-Specific Diagnosis and Visualization of Bone Micro-Structures

L. Podshivalov, A. Fischer and P. Z. Bar-Yoseph

Abstract Bone is a hierarchical bio-material whose architecture differs at each level of hierarchy and whose mechanical properties can vary considerably, even on the same specimen, due to bone heterogeneity. Because of their complexity and large number of details, these models are considered to be large-scale models. Modeling, visualization and diagnosis of such models is challenging, since a large amount of data must be processed rapidly. Moreover, if physically based modeling is required, material properties are also included in the computational model in addition to geometrical data, making the task more difficult. Therefore, advanced technology and computational methods are required for efficient, reliable and robust visualization and diagnosis. In this chapter we describe state-of-the-art technologies and methods that facilitate the processing of bone structure at the micro-scale. Specifically, we relate to computational methods that enable structural analysis of this highly detailed structure for medical diagnosis.

1 Introduction

Visualization of bone micro-structures and diagnosis of bone diseases are two interconnected processes. Visualization techniques are driven by diagnostic needs, while the diagnosis process, which utilizes emerging medical imaging technology, dictates how the bone structure should be visualized. During the last two decades,

L. Podshivalov · A. Fischer (✉)

Laboratory for CAD and LCE, Technion, Haifa, Israel

e-mail: meranath@tx.technion.ac.il

L. Podshivalov · P. Z. Bar-Yoseph

Computational Biomechanics Laboratory, Technion, Haifa, Israel

visualization methods for bone-micro structure have developed considerably for a number of reasons: (a) Recently, medical imaging technology provides high-resolution scanning that capture micro-scale structures; (b) computation and graphics techniques have developed tremendously, enabling modeling and analysis of complex models; (c) our understanding of the medical and biological processes involved in modeling and remodeling of bone tissue has improved, thus leading to new algorithms and methods for geometric modeling, analysis and visualization. In this chapter, we review the evolution of the field of patient-specific visualization and diagnosis of bone micro-structure, focusing on medical imaging technology, geometric modeling, structural analysis and visualization.

1.1 Bone Hierarchical Structure

Bones are composed of hierarchical bio-composite materials characterized by complex multi-scale structural geometry and complex behavior. The outer shell of bone is known as *cortical bone* and is characterized by its strong and dense structure. The inner structure consists of small plates and rods (in Latin *trabecula*) arranged in complex three-dimensional structures. These structures, known as called *trabecular bone*, are characterized by their high strength-to-weight ratio. For many years, scientists have been interested in this complex structure and the processes that govern its formation, regeneration and destruction throughout life. In 1892, the anatomist and orthopaedic surgeon Julius Wolff published a work in which he defined “Wolff’s Law” that predicted a relationship between the geometrical structure and mechanical properties of bone micro-structures [40]. It is known today that bone tissue structure can be classified into five structural levels, ranging from macro-scale to nano-components [60, 71]:

- Macro-structure (mm– μm): trabecular and cortical bone.
- Micro-structure (10–500 μm): osteons and trabeculae.
- Sub-microstructure (1–10 μm): lamellae and single trabecula.
- Nanostructure (100 nm–1 μm): fibrillar collagen and embedded mineral.
- Sub-nano-structure (< 100 nm): molecular structure of mineral, collagen, and non-collagenous organic proteins.

Figure 1 illustrates the hierarchical structure of bone tissue, ranging from organ-to sub-nano-scale. Depending upon the anatomical site, bone architecture differs significantly at the micro-structural level with respect to shape, thickness, element direction and size. For example, the rod-like structures at the vertebra differ significantly from the plate-like structure at the femoral head. Bone architecture can also vary at different locations on the same site as a result of functionality and locally applied forces characterized by magnitude and direction. Thus, each patient’s bone structure is unique and is influenced by gender, age, and physical condition.

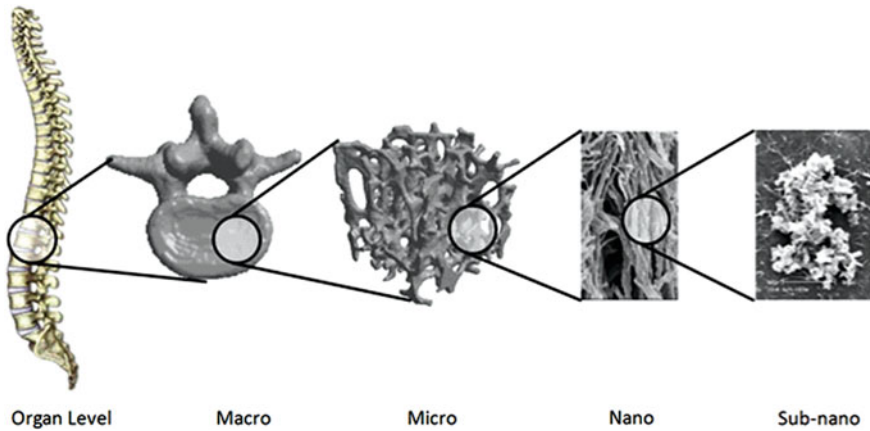


Fig. 1 Hierarchical structure of bone tissue (*from left to right*): spine, vertebra bone, trabecular bone structure, fibril array and bone crystals

As of today, due to technology limitations and limited understanding of the biological processes at other structural scales, macro-and micro-scales remain at present the only diagnostically relevant structures. Current research aims to define structure-mechanical relationships at the nano-scale [30] and to model the modeling and remodeling processes of the bone tissue at the cellular levels [41].

1.2 Diagnostic Approach

Diagnosis of bone micro-structures is especially relevant in cases of metabolic bone diseases. For example, metabolic bone diseases such as osteoporosis are characterized by micro-architectural deterioration of bone tissue, leading to micro fractures; therefore, early diagnosis at the micro-scale is a key to intervention. Current guidelines issued by the World Health Organization (WHO) define Bone Mineral Density (BMD) measurements as a default assessment tool for diagnosing osteoporosis. BMD results are reported as a T-score and a Z-score.

The T-score represents the number of standard deviations above or below the mean bone mineral density for sex and race matched to 30 year-olds. A Z-score compares the patient with a population adjusted for age, sex and race. In postmenopausal women, osteoporosis is defined as a BMD T-score of more than 2.5 standard deviations below the sex-adjusted mean for normal young adults at peak bone mass. The BMD result is used to classify patients into three categories: (a) normal; (b) osteopenic; and (c) osteoporotic. A fourth category is severe osteoporosis, which is not defined by BMD but rather by the presence of osteoporotic fractures. Patients with normal BMD values need no further therapy, osteopenic patients should be counseled and treated with preventive therapy, and

Table 1 Comparison of micro-scale medical imaging technologies

Technology	Method	Resolution	Advantages	Disadvantages
CT	pQCT	80 μm in vivo	Lower radiation than μCT method	Radiation is limited to peripheral sites
	μCT	6 μm in vitro	Highest spatial resolution for micro-structures	Unacceptably high radiation doses for human use limited field of view
		50 μm in vivo	Highest in vivo resolution	Radiation
MRI	μMRI	90 μm in vivo	No radiation exposure	Long acquisition time

should receive active therapy aimed at increasing bone density and decreasing fracture risk. The most widely used techniques for assessing bone mineral density are: (a) Dual-Energy X-ray Absorptiometry (DEXA); (b) Dual Photon Absorptiometry (DPA); (c) ultrasound; and (d) Quantitative Computerized Tomography (QCT), the only technology capable of providing 3D results. Although BMD testing is commonly used, it presents a number of limitations:

- The BMD result does not describe the complex 3D bone micro-structure, but rather only offers an indication with a single scalar value.
- BMD is not applied on 3D micro-architecture.
- BMD has only 70% reliability.
- BMD is difficult to measure accurately.
- No uniform threshold exists for all instruments and sites.

Therefore, it is required to develop 3D micro-scale scanning methods from which 3D models can be constructed and analyzed.

1.3 Micro-Scale 3D Scanning Methods

Constant improvements in medical imaging technology allow high resolution in vivo scanning of large specimens or even whole bone models. These methods are: (a) peripheral Quantitative Computed Tomography (pQCT); (b) micro Computed Tomography (μCT); and (c) micro Magnetic Resonance Imaging (μMRI). All are based on the common technology of CT and MRI. Table 1 compares the existing 3D imaging methods. While CT-based micro-scale imaging technology provides higher spatial resolution than μMRI technology, the major advantage of μMRI lies in the absence of ionizing radiation.

These scanning technologies have become popular due to the development of new 3D computerized methods for the reconstruction of trabecular structure from micro CT and MRI images [5, 13] as well as to the increase in computational resources that has led to the development of analytical tools for structural and mechanical analysis.

Prior to diagnosis, medical images must be processed and a geometric model must be reconstructed. In following section the geometric methods for model reconstruction are presented.

2 Volumetric Model Reconstruction from μ CT/ μ MRI Images

The first step in processing μ CT/ μ MRI images of scanned tissue for diagnosis is to reconstruct the 3D geometric model from the medical images. 3D model reconstruction can be divided into two main categories: volumetric reconstruction and surface reconstruction. Subsequently, even if the geometry of a reconstructed model is of high visualization quality, the issue of mesh quality is handled through remeshing that enables further analyses, such as finite element analysis.

2.1 *Methods for Geometric Model Reconstruction from CT/MRI Imaging*

Methods for model reconstruction from micro-CT/MRI imaging, which is used today, are mainly based on traditional methods for macro-scale models. The following describes the most common methods for reconstructing macro-scale medical models from CT/MRI imaging.

2.1.1 Surface Reconstruction Methods for Macro-Scale Models

Existing approaches for surface reconstruction can be classified into two main categories: (a) Marching Cubes method; and (b) Reconstruction from parallel cross-sections.

Marching Cubes method: The most well-known method for surface reconstruction of 3D models from medical images is the Marching Cubes method developed by Lorensen and Cline in 1987 [46]. The output of this method is a surface model with triangulated mesh. The triangulation is achieved via a look-up table that defines all possible surface-edge intersections resulting from the vertex value (tissue or void). Although this method was considered revolutionary for its time, it is prone to creating inner holes. Since then, numerous enhancements and variations to this method have been published and implemented [3, 50, 51]. The main disadvantage of this method is that it generates unsmooth and step-like surfaces.

Reconstruction from parallel cross-sections: Surface reconstruction from μ CT/ μ MRI images, defined as parallel cross-sections, yields a 3D triangulation model. One of the early works in this area was published by Keppel in 1975 [44] and provided a solution for a limited case in which each slice contains only

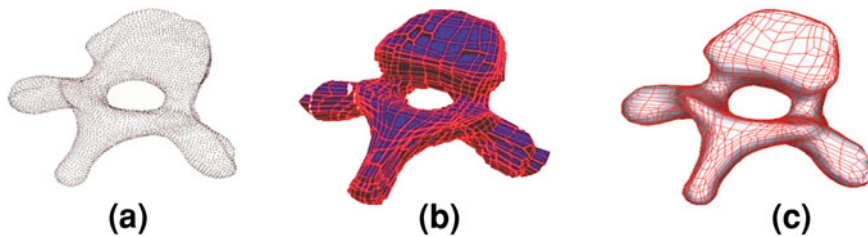


Fig. 2 Anisotropic grid-base volumetric reconstruction of vertebra. **a** Cloud of points retrieved from medical images. **b** Volumetric reconstruction using hexahedral elements. **c** Surface reconstruction using quads [5, 6]

one contour. In 1978, Christiansen and Sederberg [18] extended this method to dual contours. In the 1990s, increased use of CT and MRI technology for medical diagnosis gave this research area a boost. A large number of studies have been published that consider reconstruction of organs and systems with high geometrical complexity, such as the cardiac system and the brain [7, 17, 19]. One major contributor to research on surface reconstruction from parallel cross-sections is Prof. Barequet, who has published numerous works on this subject [9]. Recent research focuses on reconstruction from sparsely sampled parallel contours [53] and nested contours [8].

2.1.2 Volumetric Reconstruction Methods for Macro-Scale Models

Existing approaches to volumetric reconstruction can be classified into two main categories: (a) Grid-based method; and (b) Anisotropic grid-based method.

Grid-based method: This approach to 3D model reconstruction from medical images is based on direct conversion of pixels into hexahedron elements (voxels). This approach is widely used by the biomedical community for μ FE analysis of bone micro-structure [4, 61, 67, 68], despite its disadvantage in the form of jagged edges on the envelope. In 2006, Boyd and Müller [13] published a smoothing algorithm for this type of elements, but the resulting surface still lacks natural smoothness. The grid-based method can be also used for creating a tetrahedral elements for finite element analysis, as in the work of Frey et al. [24]. This approach was used in early studies of μ FE of bone micro-structure [66].

Anisotropic grid-based method: Another approach for volumetric reconstruction is based on anisotropic grid-based techniques [5, 48]. The main idea of this method is first to construct a geometric field, which is induced by the shape of the surface. This geometric field represents the natural directions and grid cell size for each point in R^3 . Then, the imposed volumetric grid is deformed toward the object's shape according to the produced geometric field. This method produces models in which the basic volumetric unit can be either a hexahedron or a tetrahedron (Fig. 2a-c).

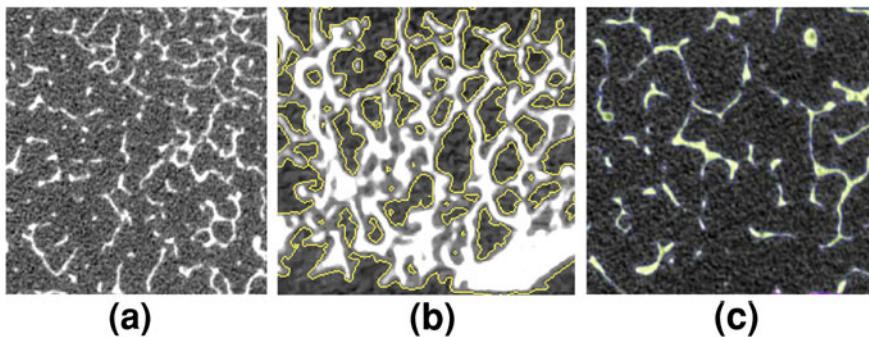


Fig. 3 Segmentation process of micro-CT images. **a** Original image. **b** Segmentation with incorrect thresholds. **c** Segmentation with correct thresholds

In the case of reconstruction from μ CT/ μ MRI images, the above methods cannot be applied directly due to the large number of details and to the fact that high-resolution images are often noisy, as depicted in Fig. 3a. Therefore, more reliable filtering and segmentation methods are needed. Good segmentation requires choosing threshold values of the Hounsfield Units (HU) that optimally separate the bone micro-structure from the bone marrow. A threshold range that is too wide can lead to segmentation that includes bone marrow and interconnects between separated parts, as shown in Fig. 3b and c depicts segmentation results achieved with precise threshold values. In this case, curvature filter [47] and 3D bilateral filter [48] were applied to the original image prior to segmentation. Such filtering smooths the images and eliminates the noisy background and preserves features.

2.2 Domain-Based Approach for Reconstruction from μ CT/ μ MRI Imaging

To facilitate fast computational performance and obtain a mesh that can be easily handled for later optimization and visualization, a domain-based approach is desired for parallel computation of large-scale problems. The problem domain is subdivided into sub-domains on which the physical problem is computed in parallel. Each sub-domain contributes to the global solution of the problem. The subdivision into sub-domains can be grid-based, can utilize a load-balancing approach by means of graph partition, e.g. Metis [42] or can be subdivided into simple sweepable volumes using Voronoi graphs [64].

There are two main domain decomposition approaches for interaction between sub-domains: overlapping and non-overlapping methods. The first approach, known as the Schwarz Method, subdivides the space into overlapping sub-domains. This approach is practical for problems in which the global domain can be constructed from sub-domains with simple geometric shapes. The domains can

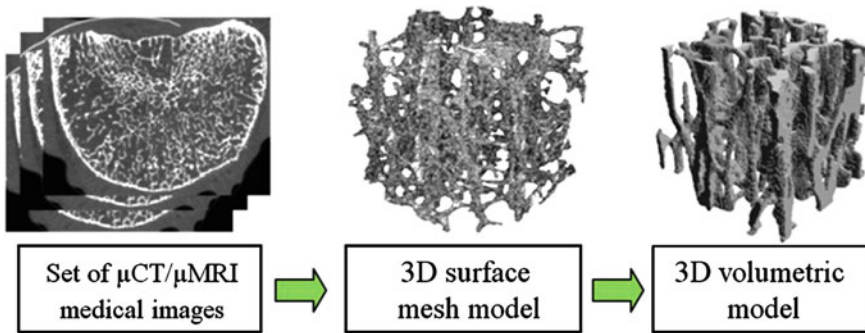


Fig. 4 Main stages in physically based multiscale modeling of large-scale porous structures

be solved in parallel, where the boundary values of the overlapped regions are updated after each iteration. The second approach subdivides the space into adjoining sub-domains, thus requiring that one sub-domain be solved prior to solving the next one or that the *ghost nodes approach* be used. Both types of domain decomposition methods facilitate the solution of complex problems by means of parallel computing. In case of processing of medical images, a non-overlapping method with grid-based subdivision can be utilized (Fig. 4).

Each sub-domain must capture the trabecular structure of the analyzed bone. In the field of image processing, the Nyquist sampling rate [28] defines the minimum spatial frequency required for correct sampling of the image. According to the Nyquist sampling rate, the sampled interval must be at least two times smaller than the size of the smallest detail to be captured. If the smallest detail is represented by the sum of morphological parameters, trabecular thickness ($Tb.Th$) and trabecular spacing ($Tb.Sp$) of the model, then the minimum size of sub-domain should be at least $2 \times (Tb.Th + Tb.Sp)$. According to Hildebrand et al. [32], the average values for $Tb.Th$ and $Tb.Sp$ are 0.3 mm and 0.8 mm, respectively. Thus, a sub-domain of 128^3 voxels (4.7 mm^3) in size with a spatial resolution of $37 \text{ }\mu\text{m}$, as used in this work, included on average $4 \times (Tb.Th + Tb.Sp)$.

2.3 From Surface Triangular Mesh to Volumetric Hexahedral Model

If the surface reconstruction approach is used, the surface model needs to be converted into a volumetric model. A voxelization technique can be utilized for this conversion. Voxelization can be carried out using different methods. Not all methods can deal with complex 3D geometry, so that structural information may be lost in the process. The voxelization method that provided the most optimal results is based on the flood-fill approach [49]. Flood-filling begins with a seed voxel, identified by stepping a short distance along the inward-pointing surface normal of a mesh triangle. This voxel is marked as an *internal voxel*. Then, a ray is

cast recursively from each *internal voxel* to all its neighbors. If the ray does not cross the surface, the neighbor is marked as an internal voxel. If the ray does cross the surface, the neighbor is marked as a *border voxel*. The process is terminated when all *internal voxels* were handled.

2.4 Hierarchical Multiresolution Geometric Modeling

The resulted volumetric model can be used for structural analysis. However, such a model is still impractical for the majority of applications. For efficient mechanical analysis or even visualization, parallel processing is required. Such technology does not typically exist at medical centers, and thus an alternative approach is required. One of the recent approaches utilizes hierarchical multiresolution geometric modeling. It is useful for making storage, transmission, computation, and visualization of these models feasible and more efficient. Multiresolution modeling algorithms are also known as simplification algorithms [54]. They can be applied to surface meshes and grid-based volumetric structures. In the field of surface mesh representation, the *edge-collapse* approach proposed by Hoppe et al. [39] is the most common decimation operation. Edge contraction operates on a single edge and contracts the edge to a single vertex. *Edge collapse* is a reversible operation. The inverse of this operation is known as *vertex splitting*. Progressive Meshes (PM) [38] are built by considering a sequence of edge collapses that iteratively simplify a mesh. The original mesh M may be obtained from the base mesh M_0 through progressive refinement by applying all the vertex split updates in the sequence. If only part of the sequence is applied, a model at an intermediate level-of-detail (LOD) is obtained. Volumetric multiresolution algorithms have hierarchical characteristics that allow continuous bi-directional transition from a smooth macro-scale model to a porous micro-scale model [57]. The most prevalent 3D hierarchical multiresolution geometric data structure is the octree whose common property is the principle of recursive decomposition of space by a factor of eight [63], as depicted in Fig. 5a.

In octree, each node stores an explicit three-dimensional point, which is the center of the subdivision for that node. The root node of the octree represents a finite bounded space, so that the implicit centers are well-defined. A 3D hierarchical geometric model allows continuous transition from a smooth macro-scale model with low topological complexity to a trabecular micro-scale model with high topological complexity. The intermediate levels are equivalent to zooming from a dense trabecular structure to sub-group of trabeculae, and finally to a singular trabecula. The octree structure enables fast transition between different structural levels of bone model. Moreover, due to the domain-based approach, a high-resolution model can be straightforwardly presented at the *Volume of Interest (VOI)* while keeping the rest of the model at low resolution. The octree data structure and an example for macro-and micro scale vertebra models are depicted in Fig. 5b–e. Figure 6 shows the geometric differences at different levels of the

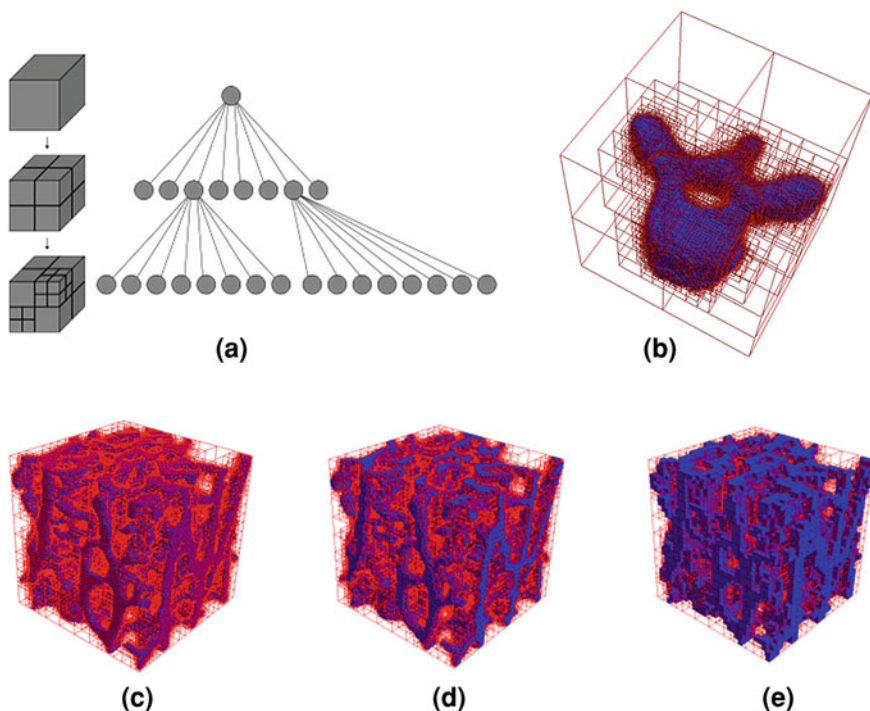


Fig. 5 Hierarchical modeling utilizing octree data-structure. **a** Recursive subdivision of a cube into octants and its corresponding octree. **b** The octree modeling of vertebra at the macro-scale. **c–e** Different resolutions of the octree representation of a sub-domain at the micro-scale level, 128^3 , 64^3 and 32^3 resolutions respectively [58]

hierarchical octree representation. Although the global appearance of the model generally seems identical, detailed observation reveals distinctions, as seen in the zoomed regions. The dominant features of the structure have been maintained but at a higher resolution level, and minor features appear as well. These features are essential when an accurate representation of the bone micro-structure is desired.

It is important to emphasize that the multiresolution approach handles only the geometrical aspects of a model and does not take into account its physical properties, such as weight, density, elasticity and conductivity. Without these properties, the model loses its physical substance at the intermediate levels and cannot be used for mechanical analysis.

3 Structural Bone Analyses for Patient-Specific Diagnosis

Over the years, the challenge to understand how bone micro-structure influences the development and progress of metabolic bone diseases has attracted many researchers. Their research concentrated mainly on two areas: (a) development of

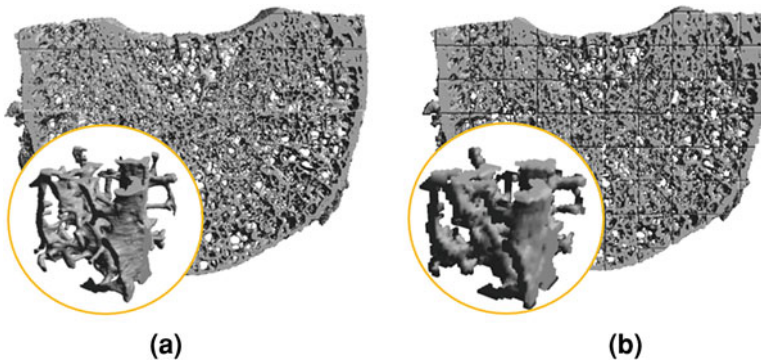


Fig. 6 : Multiresolution geometric modeling of trabecular bone with voxel size of (a), 37 μm and (b) 148 μm

structural parameters that can be retrieved initially from the medical images and later from the reconstructed volumetric models, and (b) structural mechanical analysis of bone utilizing finite element methods.

3.1 Extracting 3D Bone Structural and Topological Parameters

In the 1970s, X-rays and CT-based imaging technology allowed acquiring images on which micro-scale structure was recognizable. This led to the development of a set of structural parameters, some of which are used till today. Table 2 provides a partial list of these parameters. Two types of 3D parameters have been determined by commercial systems and in the literature: structural and topological. Structural parameters are based on geometric properties of the model alone, while topological parameters take into consideration bone connectivity and topology.

- (a) *Basic parameters*: These basic parameters are used for estimating the surface (BS) and volume (BV) of bone tissue [23]. These parameters have characteristic values at each anatomical site and thus can be used for quantification of bone quantity.
- (b) *Trabecular architecture descriptors*: This set of parameters describes the trabecular architecture of the bone, which can vary between two main structures: a rod-like structure characteristic of vertebrae, and a plate-like structure characteristic of femoral bone. These parameters are used for estimating trabecular thinning, measuring marrow cavity and evaluating number of plates per unit length. Originally these parameters were approximated by using a set of the basic parameters, assuming plate-like architecture [23], but currently their values can be calculated directly from a 3D model [32, 33].

Table 2 3D bone structural and topological parameters

Type	Group	Parameter	Notation
Structural parameters	Basic parameters	Bone surface	BS
		Bone volume	BV
	Trabecular architecture descriptors	Trabecular thickness	Tb.Th
		Trabecular separation	Tb.Sp
		Trabecular number	Tb.N
	Advanced structural descriptors	Marrow star volume	Ma.St.V
		Structure model index	SMI
		Percent plate	%Plate
	Anisotropy descriptors	Degree of anisotropy	DA
		Percent bone in load direction	%Bone _{LD}
Topological parameters	The connectivity descriptor	Connectivity density	ConnD
	Process descriptors	Surface-to-curve ratio	S/C
		Erosion index	EI

- (c) *Advanced structural descriptors*: The Marrow Star Volume parameter (Ma.St.V) can be used to describe the “voids” within the trabecular structure. It is a sensitive descriptor for quantifying bone loss either through trabecular thinning or loss of entire trabecula [12]. Alternatives for the trabecular number parameter include a Structure Model Index (SMI) [34], which varies from 0 to 3 (an ideal plate structure and an ideal rod-like structure, respectively), and Percent Plate (%Plate), which allows quantitative estimation of the effect of bone resorption on the shape of the trabecula.
- (d) *Anisotropy descriptors*: Degree of Anisotropy (DA) [29] and Percent Bone in Load Direction (%Bone_{LD}) [12] are used to describe the anisotropy of the trabecular bone structure. The DA parameter is used for defining the direction of the preferred orientation of trabeculae and is important for directionally dependent mechanical properties. The %Bone_{LD} parameter allows quantitative estimation of the effect of bone resorption on the shape of the trabeculae.
- (e) *The connectivity descriptor*: The Connectivity Density (ConnD) parameter [55] provides an estimate of the number of trabecular connections per mm³. It is defined as the number of trabecular elements that may be removed without separating the network and is frequently referenced as the parameter mostly affected during the progression of osteoporosis [56].
- (f) *Process descriptors*: Topologically based parameters for evaluation and characterization of bone micro-architecture have been defined [27, 69]. These parameters are used to provide detailed insight into the 3D trabecular network topology [70]. Estimation of these parameters is based on digital topological analysis that classifies each voxel according to its connectivity with the neighboring voxels. As a result, a number of powerful discriminators of different structural arrangements are defined. The first is the

surface-to-curve ratio (S/C), which is expected to be a sensitive indicator for the conversion of plates to rods. The second is the Erosion Index (EI), defined as the ratio of the sum of parameters expected to increase upon osteoclastic resorption (edges), divided by the sum of parameters expected to decrease due to such processes (surface).

The above parameters have provided better understanding of bone micro-structure; however, their estimation is limited to the available technology. Since digital image analysis was not initially available, most of the parameters were approximated from two basic parameters—BS and BV. Moreover, even the precision of these two parameters was dictated by the resolution of imaging technology. Nowadays, most of these parameters have already been integrated into commercial applications provided with μ CT and μ MRI scanners. However, they yield only implicit and partial descriptions of bone topology, structure and geometric properties (shape elements and orientation). Therefore, a complete 3D micro-structural mechanical analysis is preferable.

3.2 Finite Element Mechanical Analysis of Bone Micro-Structures

Along with parametric structural analysis, researchers began utilizing finite element mechanical analysis for estimating bone strength and predicting its condition. Mechanical analysis was initially restricted to the macro-scale [14, 16], and material properties were evaluated by applying the homogenization approach. The homogenization theory was developed to analyze the physics of micro-structured materials [11] and has been used extensively to analyze composite materials and predict optimal topology of micro-structured materials [10]. The method has also been used to predict the influence of trabecular bone architecture on effective stiffness and to estimate trabecular tissue stress and strain for arbitrary global loading [36, 37]. The homogenization methods allow replacing complex biological models with their respective simplified macro models that can be solved with ordinary computer resources. However, the asymptotic method is valid only when there is an order of magnitude difference between two consecutive levels, while the RVE method represents the complex geometric structure with a solid model. Averaging the micro-scale structure and replacing it with a solid model that has equivalent material properties lead to a loss of structural information that is important for precise diagnosis.

During the 1980 and 1990s, the growth in computational resources and in the availability of parallel computing has created two trends in the area of computational mechanics: (a) an increase in the number of elements in analyzed models and (b) a decrease in the size of these elements, leading to an increase in the overall number of degrees of freedom. The combination of these two trends has led to the development of large-scale computational models, known as micro Finite Element Analysis techniques (μ FEA) [68]. Initially, the solution utilized the

element-by-element precondition conjugate gradient (EBE-PCG) method [15, 26] and was executed on super-computers, e.g. Cray.

In the 2000s, modern algebraic multi-grid (AMG) linear solvers have been utilized for solving large-scale FE trabecular models with nearly half a billion degrees of freedom for a vertebra [2] and for the distal part of the radius of a human forearm [4], both with spatial resolution of 30 μm . The solution required state-of-the art parallel FE applications and thousands of processors. Indeed, analyses of high resolution models require considerable computational resources that are not commonly available at hospitals and medical centers. Thus, a multi-scale finite element analysis method was proposed.

3.3 Multiscale Finite Element Analysis of Bone Micro-Structure

Multiscale methods are an extension of the multiresolution approach, which integrates material properties with the geometrical method. In engineering, multiscale methods are used mainly for analysis, as they are intended to bridge between different structural levels. Yet state-of-the-art multiscale methods do not support continuous transition between consecutive structural methods and only allow discrete hierarchical modeling, assuming order of magnitude differences between these levels, e.g. macro-, micro- and nano levels. Most state-of-the-art multiscale methods utilize multi-step homogenization [25, 31, 52] or mesh superposition [43]. These methods assume order-of-magnitude scale separation between two consecutive levels of hierarchy. Therefore, continuous transition in terms of geometrical modeling and mechanical properties is not available.

Currently there are two main computational models in engineering: a homogenized macro-scale model in which the highly detailed structure is replaced with one that is homogeneous, and a high-resolution micro-scale model without intermediate models. The classic homogenization procedure is based on the asymptotic or Representative Volume Element (RVE) method [1, 72]. The homogenization theory was developed to analyze the physics of micro-structured materials [11] and has been used extensively to analyze composite materials and predict optimal topology of micro-structured materials [10]. Homogenization methods allow replacing complex biological models with their respective simplified macro models that can be solved with ordinary computer resources. However, the asymptotic method is valid only when there is an order of magnitude difference between two consecutive levels, while the RVE method represents the complex geometric structure with a homogeneous model. This approach has been used for physically-based modeling of deformable elastic inhomogeneous models for medical applications [45], surgery simulation and animation [22].

The proposed multiscale domain-based approach [59] enables using a “digital magnifying glass” for continuous transition between macro- and micro-scales, as illustrated in Fig. 7. This computational tool can be used by engineers for solving complex models on commonly available workstations rather than on

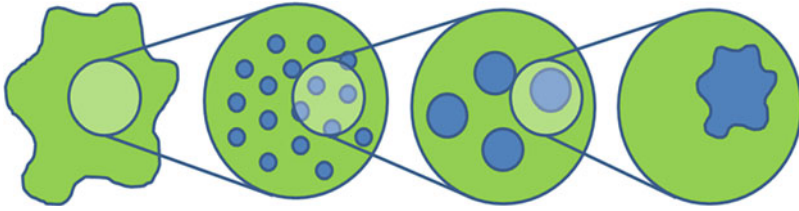


Fig. 7 Schematic representation of the continuous multiscale method

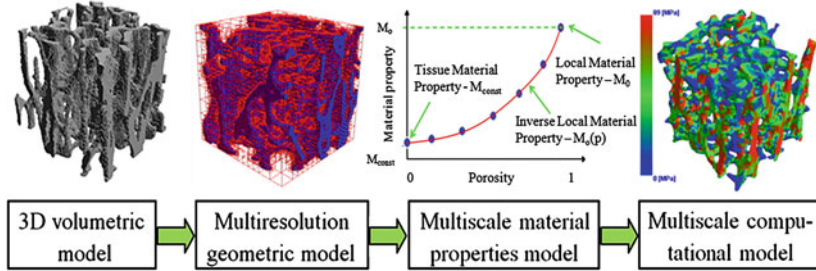


Fig. 8 Main stages of the presented physically based multiscale modeling for large-scale porous structures

super-computers or grid-based systems. The approach is based on the following stages: (a) creation of a volumetric geometric model from a surface model or set of image slices; (b) generation of a multiresolution geometric model using hierarchical data structure; (c) evaluation of a multiscale material properties model; and (d) integration between the geometric and material properties models. Figure 8 depicts these stages, as described below.

Realizing the proposed multiscale approach requires synergy between the multiresolution geometric model and the assignment of *local mechanical properties* at each intermediate scale. The local mechanical properties vary at each intermediate scale due to changes in the geometric model. The main aim at this stage is to preserve the *effective (global) material properties*. Once the effective property to be preserved is selected, the *local material properties* model can be established.

A trivial illustration of the proposed method would be to keep the weight (m) of a model as invariant. Then for an intermediate model of volume V_i the local density ρ_i of the material must be evaluated to guarantee that:

$$V_i \cdot \rho_i = m = \text{const} \quad (3.1)$$

A similar approach can be utilized for evaluation of different material properties. However, several effective material properties also depend on structural or topological information of the model, e.g. stiffness and conductivity. Thus, a preprocessing stage for estimating these properties is necessary. Following is a

description of a method for estimating local material properties for intermediate models, assuming a linear elasticity model with small displacements [58]:

Stage 1: Estimate the effective material properties for a set of intermediate models without changing the local material properties. This set must include the model with the highest available resolution.

The elasticity model is represented by the generalized Hooke's law that defines the relationship between the dimensionless displacements applied to the model (strains- ε) and the forces per area (stresses- σ) developed in the material:

$$\sigma_{ij} = C_{ijkl}\varepsilon_{kl} \quad (3.2)$$

where C_{ijkl} are fourth-degree tensor constants that construct the material stiffness matrix.

For homogenization of material properties, the RVE formulation can be used. Applying the RVE homogenization establishes a relation between the average values of stresses ($\bar{\sigma}$) and strains ($\bar{\varepsilon}$). For the representative volume V these values are defined as:

$$\bar{\varepsilon} = \frac{1}{V} \int_V \varepsilon dV \quad \bar{\sigma} = \frac{1}{V} \int_V \sigma dV \quad (3.3)$$

The boundary conditions are applied in terms of displacements u_i :

$$u_i = \varepsilon_{ij}^0 x_j \quad (3.4)$$

where ε_{ij}^0 are constant strains and x_j are point coordinates.

The average strain values for the above boundary conditions are:

$$\bar{\varepsilon}_{ij} = \varepsilon_{ij}^0 \quad (3.5)$$

Now the elastic stiffness matrix constants can be found using (3.2). In the case of fully anisotropic material, 21 independent stiffness matrix constants must be estimated. This calculation requires performing a finite element analysis on each sub-domain with six different boundary conditions. The first three sets of boundary conditions are equivalent to uniaxial compression tests, one for each major axis. The last three are equivalent to shear tests.

Before the algorithm proceeds to the next stage, the symmetry planes of the material are found and used for transforming the stiffness matrix to its orthotropic form. Cowin and Mehrabadi [20] showed that symmetry planes exist if the eigenvectors of the matrices (3.6) and (3.7) are the same and the eigenvalues are different.

$$C'_{ijkk} = \begin{bmatrix} C'_{11} + C'_{12} + C'_{13} & C'_{16} + C'_{26} + C'_{36} & C'_{15} + C'_{25} + C'_{35} \\ C'_{16} + C'_{26} + C'_{36} & C'_{12} + C'_{22} + C'_{23} & C'_{14} + C'_{24} + C'_{34} \\ C'_{15} + C'_{25} + C'_{35} & C'_{14} + C'_{24} + C'_{34} & C'_{13} + C'_{23} + C'_{33} \end{bmatrix} \quad (3.6)$$

$$C'_{ikkj} = \begin{bmatrix} C'_{11} + C'_{55} + C'_{66} & C'_{16} + C'_{26} + C'_{45} & C'_{15} + C'_{46} + C'_{35} \\ C'_{16} + C'_{26} + C'_{45} & C'_{22} + C'_{44} + C'_{66} & C'_{24} + C'_{34} + C'_{56} \\ C'_{15} + C'_{46} + C'_{35} & C'_{24} + C'_{34} + C'_{56} & C'_{33} + C'_{44} + C'_{55} \end{bmatrix} \quad (3.7)$$

To find the eigenvectors of these matrices, the SVD decomposition is applied. The eigenvectors are further used as vectors of the rotation matrix Q for tensor transformation from anisotropic to orthotropic material tensor. After the tensor transformation is applied, the orthotropic material stiffness matrix C_{ijkl} is generated:

$$\bar{\sigma} = C \cdot \bar{\varepsilon} = \begin{bmatrix} \sigma_{11} \\ \sigma_{22} \\ \sigma_{33} \\ \sigma_{23} \\ \sigma_{31} \\ \sigma_{12} \end{bmatrix} = \begin{bmatrix} C_{11} & C_{12} & C_{13} & 0 & 0 & 0 \\ C_{21} & C_{22} & C_{23} & 0 & 0 & 0 \\ C_{31} & C_{32} & C_{33} & 0 & 0 & 0 \\ 0 & 0 & 0 & C_{44} & 0 & 0 \\ 0 & 0 & 0 & 0 & C_{55} & 0 \\ 0 & 0 & 0 & 0 & 0 & C_{66} \end{bmatrix} \cdot \begin{bmatrix} \varepsilon_{11} \\ \varepsilon_{22} \\ \varepsilon_{33} \\ \varepsilon_{23} \\ \varepsilon_{31} \\ \varepsilon_{12} \end{bmatrix} \quad (3.8)$$

Currently, nine independent material properties of the orthotropic material can be calculated using the generalized Hooke's law in stiffness form.

The calculated orthotropic material properties are:

$$E_{11} \quad E_{22} \quad E_{33} \quad G_{23} \quad G_{31} \quad G_{12} \quad \nu_{23} \quad \nu_{31} \quad \nu_{32} \quad (3.9)$$

where: E_{ii} -Young's modulus, G_{ij} -shear modulus and ν_{ij} -Poisson's ratio.

Stage 2: Define a correlation between the geometric properties of the intermediate models (e.g. porosity) and their respective *effective material properties*. The correlation between the porosity (p) and the *effective material properties* (M) can be established in terms of a polynomial function. Coefficients of the polynomial (a_i) can be found straightforwardly by solving a set of linear equations. After computing all the coefficients, a common factor can be extracted from the equation and rewritten as follows:

$$M(p) = M_0 \cdot \sum_{i=n}^0 \hat{a}_i p^i \quad (3.10)$$

where M_0 represents the initial *local material property*.

Stage 3: Find an inverse local material properties model that preserves the effective material properties at a constant value (M_{const}) for different intermediate models. According to the above, (3.10) can be rewritten as:

$$M_0(p) = M_{const} \cdot \left[\sum_{i=n}^0 \hat{a}_i p^i \right]^{-1} \quad (3.11)$$

In this work, the material properties at the highest resolution (micro-scale) are assumed to be isotropic. However, the geometry changes are at lower (coarser) resolutions, so orthotropic local material properties are applied to compensate for

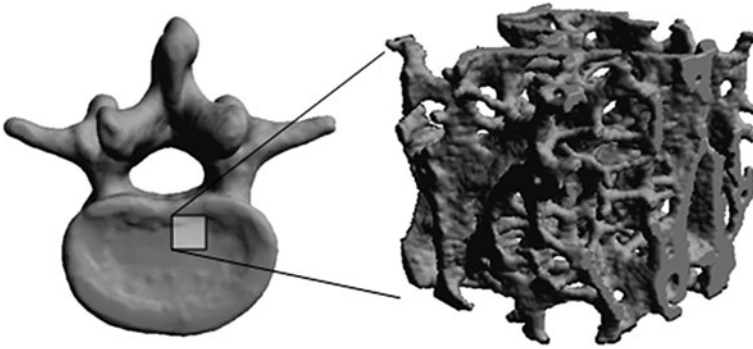


Fig. 9 Vertebra models at different scales: macro-scale on the *left* and micro-scale on the *right*

such structural changes. In effect, when the structure of the geometrical model changes from micro to macro, the geometric anisotropy is replaced by anisotropic material properties.

Stage 4: Verify the computational model by comparing the property of the intermediate models to the known and measurable property of the highest resolution model. For example, models that are used for structural mechanical analysis may be compared in terms of strain energy.

The feasibility of the proposed multiscale domain-based method has been demonstrated on a bio-medical model of L3-vertebra trabecular bone at the micro-scale structural level. Bones are bio-composite materials characterized by complex multiscale structural geometry and complex behavior, as shown in Fig. 9. Depending on the anatomical site, bone architecture differs significantly at the micro-structural level with respect to shape, thickness, direction and porosity. For example, the rod-like structures of the vertebrae differ significantly from the plate-like structure of the femoral head. Bone architecture can also vary at different locations on the same site due to functionality and locally applied forces characterized by magnitude and direction. Thus, the bone structure of each patient is unique. These characteristics are crucial for diagnosis of bone metabolic disease.

The performance of the multiscale model is demonstrated in Fig. 10. In this example, each model is analyzed with its local material properties, estimated according to the proposed method. The colors represent stresses, as each model was subjected to uniaxial compression. The stress locations are consistent for all levels of resolution. In addition, the “digital magnifying glass” approach can be easily identified. The prominent features of the model are visible at all levels of resolution. The analysis shows that the multiscale method performs according to expectations. The prominent geometric features of the micro-scale models are preserved at all levels of resolution. Moreover, the computational models are reliable and robust for all intermediate levels.

The domain-based approach improves the performance of the hierarchical multi-resolution model and the finite element mechanical analysis. The worst-case

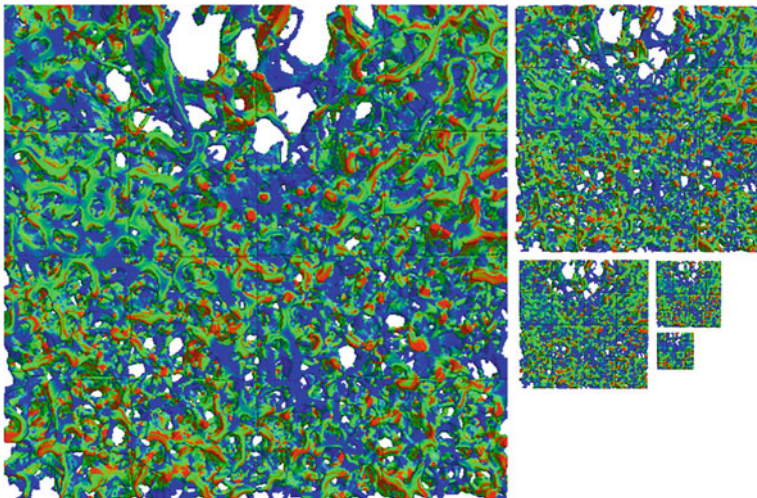


Fig. 10 View-dependent presentation of multiscale mechanical analysis, where colors represent stress intensity

time complexity of the linear octree construction algorithms is evaluated as follows.

Let N be the total number of material voxels and d the number of hierarchy levels of the octree. Encoding a material voxel model requires computational time proportional to the depth d ; encoding a region including condensation requires $O(dN)$. An adjacent voxel can be found in $O(d)$. Utilizing the domain-based approach decreases both the number of full voxels and the number of hierarchy levels required to represent them. Assuming that the maximum number of levels in the octree is $d = \log N$ and the number of sub-domains is m , the finite element solver is based on the preconditioned conjugate gradient method (PCG). The dominant operations during iterations are matrix-vector products. In general, matrix-vector multiplication requires $O(k)$ operations, where k is the number of non-zero entries in the matrix. For many problems, including FE analysis, the A matrix is sparse and $kO(N)$. Distributing this task among a number of processors significantly improves algorithm performance and allows solution of models that could not be solved otherwise.

4 Visualization of Bone Micro-Structures

As stated, visualization is not an end by itself but only a means for representing analysis and diagnosis results to physicians or orthopedists. As in geometric modeling, two different representations can be utilized for visualization-surface or volumetric. Since the volumetric model already exists, it seems natural to use a volume for visualization, though there are pros and cons to this approach:

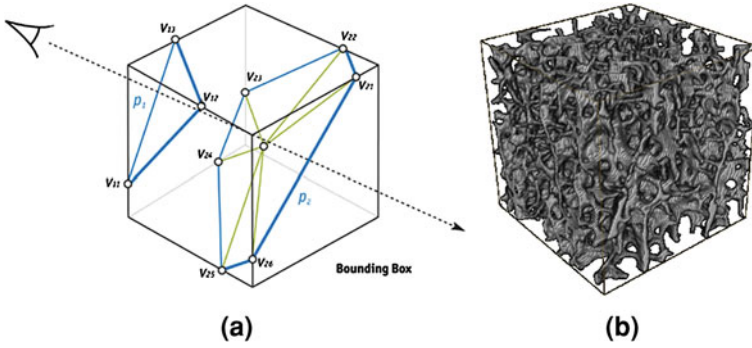


Fig. 11 Visualization of bone micro-structure utilizing direct volume method

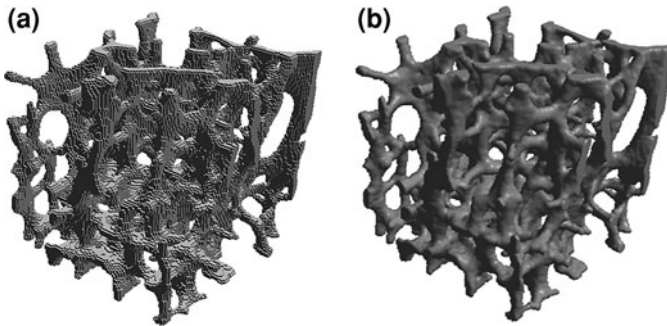


Fig. 12 Visualization of bone micro-structure using only boundary voxels and gradient kernel for calculation of model normal vectors

- Volume visualization methods require special graphic hardware that is not available on commonly used PCs. To overcome such a difficulty, the majority of visualization algorithms utilize texture mapping with a transparency parameter between different layers and blending, as depicted in Fig. 11. Modern graphic cards are designed for rapid processing of textures. Thus, this method is frequently used for volume visualization. It also enables straightforward visualization of multi-layer models, e.g. the human skeleton with different tissues. The main disadvantage of this method is that it is view dependent. Such a process is memory consuming, and its outcome is not always exact and seamless for the viewer.
- For volume representation, hexahedral elements (voxels) are usually utilized. If only surface information is of interest, then just the boundary voxels can be displayed. However, direct voxel visualization will result in jagged surfaces, as depicted in Fig. 12. Calculating model normal vectors using a gradient kernel can overcome this problem. This method permits rapid visualization of cross-sections aligned in the directions of major axes, Fig. 13. But representing a

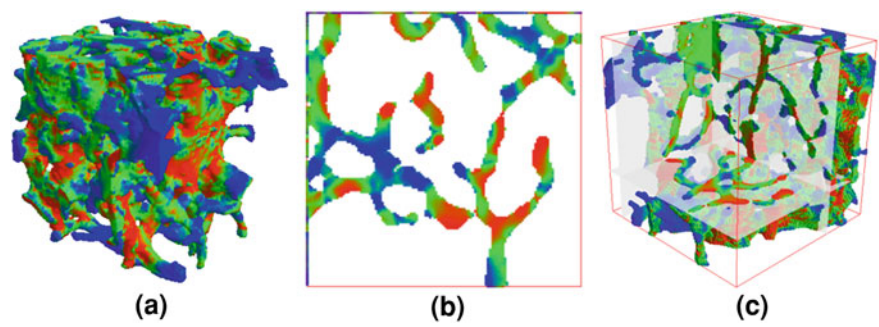


Fig. 13 Visualization possibilities using voxel representation. **a** FE analyzed model. **b** Cross-section of the model. **c** A clipped region of the analyzed model

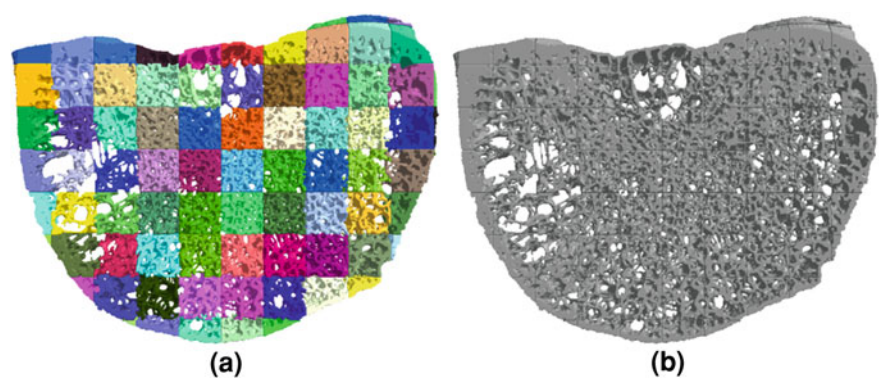


Fig. 14 Domain-based visualization of bone micro-structures. **a** Color coded sub-domains of the model. **b** The result as presented to the user

cross-section in any other direction is challenging since it requires creating an approximated plane.

The above limitations can be overcome by transforming the volumetric representation to a surface representation, for example utilizing the Marching Cubes algorithm. Surface representation will be smooth and will not require large resources for its visualization. The main disadvantage of this approach is being transformation dependent. Creating a cross-section will require recalculation of the entire surface.

Another difficulty associated with visualizing bone micro-structures relates to the large number of details in these models. Without an efficient visualization algorithm and memory resource management, such a task can be very difficult and sometimes impossible. Therefore, the domain-based approach has become popular in this field as well. Each sub-domain is prepared for visualization on a separate processor or in sequence. The user is unaware of the process since the result is seamless. An example of domain-based visualization is depicted in Fig. 14.

5 Summary and Conclusions

This chapter has reviewed the evolution of the field of patient-specific visualization and diagnosis of bone micro-structure, focusing on medical imaging technology, geometric modeling, structural analysis and visualization. State-of-the-art research focuses on a new multi-scale method that can provide a better understanding of a very complex bio-structure—bone. Moreover, a new 3D multiscale method for mechanical analysis of bone micro-structures was presented. This is one of the very few methods in the field of computational bio-mechanics that allows for the adaptive application of mechanical analysis on large-scale high resolution models. The proposed method is based on domain-based multiresolution hierarchical geometric modeling and multiscale material properties. This method incorporates the following properties:

- The hierarchical geometric model (octree) facilitates continuous bi-directional transition between micro-and macro-scale models by introducing intermediate structural levels.
- The new method for a multiscale material properties model is adapted to porosity changes at different structural levels of the geometrical model.
- The developed complete model provides the synergy between geometric and material models that is required for robust multiscale finite element analysis.

This method is aimed at assisting physicians to better understand and define bone structure strength and bone stability with respect to geometric and material properties. Medical imaging technology and common medical testing will continue to be the major diagnostic tools for initial diagnosis of the above diseases. However, different structures with similar morphological parameters may have significantly different effective material properties. As a result, one structure may withstand the applied load, while another may collapse. Therefore, mechanical testing may better predict structural behavior and improve the quality of diagnosis and prognosis, thus effectively improving patients' quality of life. Moreover, structural simulation can lead to early diagnosis prior to the appearance of symptomatic fractures. The proposed method is a new tool that can be applied to a variety of problems. We propose a number of possibilities for future applications:

- The method can be used as a diagnostic tool for estimating local bone strength in diseases that affect bone micro-structure and material properties, e.g. hypoparathyroidism [62], osteoporosis [21] and metastatic bone cancer [65]. It also can be used for local drug treatment, chemotherapy and calcium enrichment.
- Integrating topology optimization with the proposed method may lead to the design of natural micro-scaffolds [35] which can reduce the healing period.

The proposed multiscale FE method can be integrated as a module into a computerized diagnostic system that, together with other analysis tools, can make a significant impact on diagnostic conclusions. The proposed method offers an alternative to working only with existing macro-and micro-structural levels by

introducing intermediate levels. These levels provide continuous transition between macro-and micro-scales by imitating human detail perception. We believe this method can also be extended for modeling and analysis of other materials characterized by irregular and stochastic structure.

References

1. Aboudi, J.: *Mechanics of Composite Materials*. Elsevier, Amsterdam/New York (1991)
2. Adams, M.F., Bayraktar, H.H., Keaveny, T.M., Papadopoulos, P.: Ultrascale implicit finite element analyses in solid mechanics with over a half a billion degrees of freedom, proceedings of the 2004 ACM/IEEE conference on supercomputing. *IEEE. Comput. Soc.*, p 34 (2004)
3. Adriano, L.: Improving the robustness and accuracy of the marching cubes algorithm for isosurfacing. *IEEE. Trans. Visual. Comput. Graphics* **9**, 16–29 (2003)
4. Arbenz, P., van Lenthe, G., Mennel, U., Müller, R., Sala, M.: Multi-level micro-finite element analysis for human bone structures. In: Kågström, B., Elmroth, E., Dongarra, J., Wasniewski, J. (eds.) *Applied Parallel Computing*, pp 240–250. State of the Art in Scientific Computing. Springer, Berlin/Heidelberg (2010)
5. Azernikov, S., Fischer, A.: A new volume warping method for surface reconstruction. *J. Comput. Inf. Sci. Eng.* **6**, 355–363 (2006)
6. Azernikov, S., Miropolsky, A., Fischer, A.: Surface reconstruction of freeform objects based on multiresolution volumetric method. *J. Comput. Inf. Sci. Eng.* **3**, 334–338 (2003)
7. Bajaj, C.L., Coyle, E.J., Lin, K.N.: Arbitrary topology shape reconstruction from planar cross sections. *Graph. Models Image Process* **58**, 524–543 (1996)
8. Baretet, G., Goodrich, M.T., Levi-Steiner, A., Steiner, D.: Contour interpolation by straight skeletons. *Graph. Models* **66**, 245–260 (2004)
9. Baretet, G., Sharir, M.: Piecewise-linear interpolation between polygonal slices. *Comput. Vis. Image Underst.* **63**, 251–272 (1996)
10. Bendsoe, M.P., Kikuchi, N.: Generating optimal topologies in structural design using a homogenization method. *Comput. Methods Appl. Mech. Eng.* **71**, 197–224 (1988)
11. Bensoussan, A., Lions, J.L., Papanicolaou, G.: *Asymptotic Analysis for Periodic Structures*. North Holland Pub Co, Amsterdam, New York (1978)
12. Borah, B., Dufresne, T.E., Cockman, M.D., Gross, G.J., Sod, E.W., Myers, W.R., Combs, K.S., Higgins, R.E., Pierce, S.A., Stevens, M.L.: Evaluation of changes in trabecular bone architecture and mechanical properties of minipig vertebrae by three-dimensional magnetic resonance microimaging and finite element modeling. *J. Bone Miner. Res.* **15**, 1786–1797 (2000)
13. Boyd, S.K., Müller, R.: Smooth surface meshing for automated finite element model generation from 3D image data. *J. Biomech.* **39**, 1287–1295 (2006)
14. Burstein, A.H., Currey, J.D., Frankel, V.H., Reilly, D.T.: The ultimate properties of bone tissue: the effects of yielding. *J. Biomech.* **5**, 35–42, IN31-IN32, 43-44 (1972)
15. Carey, G.F., Jiang, B.N.: Element-by-element linear and nonlinear solution schemes. *Commun. Appl. Numer. Methods* **2**, 145–153 (1986)
16. Carter, D., Hayes, W.: Bone compressive strength: the influence of density and strain rate. *Science* **194**, 1174–1176 (1976)
17. Choi, Y.K., Park, K.H.: A heuristic triangulation algorithm for multiple planar contours using an extended double branching procedure. *Visual Comput.* **10**, 372–387 (1994)
18. Christiansen, H.N., Sederberg, T.W.: Conversion of complex contour line definitions into polygonal element mosaics. *SIGGRAPH Comput. Graph.* **12**, 187–192 (1978)
19. Cong, G., Parvin, B.: Robust and efficient surface reconstruction from contours. *Visual Comput.* **17**, 199–208 (2001)

20. Cowin, S.C., Mehrabadi, M.M.: On the identification of material symmetry for anisotropic elastic materials. *Q. J. Mech. Appl. Math.* **40**, 451–476 (1987)
21. Crawford, R.P., Cann, C.E., Keaveny, T.M.: Finite element models predict in vitro vertebral body compressive strength better than quantitative computed tomography. *Bone* **33**, 744–750 (2003)
22. DeBunne, G., Desbrun, M., Barr, A.H., Cani, M.P.: Interactive multiresolution animation of deformable models, Eurographics Workshop on Computer Animation and Simulation (1999)
23. Feldkamp, L.A., Goldstein, S.A., Parfitt, M.A., Jesion, G., Kleerekoper, M.: The direct examination of three-dimensional bone architecture in vitro by computed tomography. *J. Bone Miner. Res.* **4**, 3–11 (1989)
24. Frey, P., Sarter, B., Gautherie, M.: Fully automatic mesh generation for 3-D domains based upon voxel sets. *Int. J. Numer. Methods Eng.* **37**, 2735–2753 (1994)
25. Fritsch, A., Hellmich, C., Dormieux, L.: Ductile sliding between mineral crystals followed by rupture of collagen crosslinks: experimentally supported micromechanical explanation of bone strength. *J. Theor. Biol.* **260**, 230–252 (2009)
26. Fyhrie, D.P., Hamid, M.S., Kuo, R.F., Lang, S.S.: Direct three-dimensional finite element analysis of human vertebral cancellous bone, 38th meeting of Orthopaedic Research Society, Washington, DC, p 551 (1992)
27. Gombert, B.R., Saha, P.K., Hee Kwon Song, H., Wehrli, F.W.: Topological analysis of trabecular bone MR images. *Anglais* **19**, 166–174 (2000)
28. Gonzalez, R.C., Woods, R.E.: *Digital Image Processing*. Addison-Wesley Longman Publishing Co.Inc., Reading, MA (1992)
29. Goulet, R.W., Goldstein, S.A., Ciarelli, M.J., Kuhn, J.L., Brown, M.B., Feldkamp, L.A.: The relationship between the structural and orthogonal compressive properties of trabecular bone. *J. Biomech.* **27**, 375–389 (1994)
30. Gupta, H.S., Seto, J., Wagermaier, W., Zaslansky, P., Boesecke, P., Fratzl, P.: Cooperative deformation of mineral and collagen in bone at the nanoscale. *Proc. Nat. Acad. Sci.* **103**, 17741–17746 (2006)
31. Hellmich, C., Barthélémy, J.F., Dormieux, L.: Mineral-collagen interactions in elasticity of bone ultrastructure—a continuum micromechanics approach. *Eur. J. Mech.-A/Solids* **23**, 783–810 (2004)
32. Hildebrand, T., Laib, A., Müller, R., Dequeker, J., Rüegsegger, P.: Direct three-dimensional morphometric analysis of human cancellous bone: microstructural data from spine, femur, iliac crest, and calcaneus. *J. Bone Miner. Res.* **14**, 1167–1174 (1999)
33. Hildebrand, T., Rüegsegger, P.: A new method for the model-independent assessment of thickness in three-dimensional images. *J. Microsc.* **185**, 67–75 (1997)
34. Hildebrand, T., Rüegsegger, P.: Quantification of bone microarchitecture with the structure model index. *Comput. Methods Biomech. Biomed. Eng.* **1**, 15–23 (1997)
35. Hollister, S.J.: Porous scaffold design for tissue engineering. *Nat. Mater.* **4**, 518–524 (2005)
36. Hollister, S.J., Brennan, J.M., Kikuchi, N.: A homogenization sampling procedure for calculating trabecular bone effective stiffness and tissue level stress. *J. Biomech.* **27**, 433–444 (1994)
37. Hollister, S.J., Fyhrie, D.P., Jepsen, K.J., Goldstein, S.A.: Application of homogenization theory to the study of trabecular bone mechanics. *J. Biomech.* **24**, 825–839 (1991)
38. Hoppe, H.: Progressive meshes, proceedings of the 23rd annual conference on computer graphics and interactive techniques. ACM, pp 99–108 (1996)
39. Hoppe, H., DeRose, T., Duchamp, T., McDonald, J., Stuetzle, W.: Mesh optimization, proceedings of the 20th annual conference on Computer graphics and interactive techniques. ACM, Anaheim, CA, pp 19–26 (1993)
40. Huiskes, R.: If bone is the answer, then what is the question? *J. Anat.* **197**, 145–156 (2000)
41. Isaksson, H., Gröngroft, I., Wilson, W., van Donkelaar, C.C., van Rietbergen, B., Tami, A., Huiskes, R., Ito, K.: Remodeling of fracture callus in mice is consistent with mechanical loading and bone remodeling theory. *J. Orthop. Res.* **27**, 664–672 (2009)
42. Karypis, G.: METIS: a family of multilevel partitioning algorithms, University of Minnesota, USA (1998)

43. Kawagai, M., Sando, A., Takano, N.: Image-based multi-scale modelling strategy for complex and heterogeneous porous microstructures by mesh superposition method. *Modell. Simul. Mater. Sci. Eng.* **14**, 53–69 (2006)
44. Keppel, E.: Approximating complex surfaces by triangulation of contour lines. *IBM J. Res. Dev.* **19**, 2–11 (1975)
45. Kharevych, L., Mullen, P., Owhadi, H., Desbrun, M.: Numerical coarsening of inhomogeneous elastic materials. *ACM Trans. Graph.* **28**, 1–8 (2009)
46. Lorensen, W.E., Cline, H.E.: Marching cubes: a high resolution 3D surface construction algorithm. *SIGGRAPH Comput. Graph.* **21**, 163–169 (1987)
47. Malladi, R., Sethian, J.A.: Image processing via level set curvature flow. *Proc. Natl. Acad. Sci. USA* **92**, 7046–7050 (1995)
48. Miropolsky, A., Fischer, A.: Extended geometric filter for reconstruction as a basis for computational inspection. *J. Manuf. Sci. Eng.* **131**, 1–8 (2009)
49. Morris, D.: Automated Preparation Calibration and Simulation of Deformable Objects. Stanford University Department of Computer Science, Stanford/CA (2007)
50. Newman, T.S., Yi, H.: A survey of the marching cubes algorithm. *Comput. Graphics* **30**, 854–879 (2006)
51. Nielson, G.M., Hamann, B.: The asymptotic decider: resolving the ambiguity in marching cubes, *Proceedings of the 2nd conference on Visualization '91*. IEEE Computer Society Press, San Diego, California, pp 83–91 (1991)
52. Nikolov, S., Raabe, D.: Hierarchical modeling of the elastic properties of bone at submicron scales: the role of extrafibrillar mineralization. *Biophys. J.* **94**, 4220–4232 (2008)
53. Nilsson, O., Breen, D., Museth, K.: Surface reconstruction via contour metamorphosis: an Eulerian approach with lagrangian particle tracking. In *Proc. IEEE Visualization*, 407–414 (2005)
54. Nowak, M.: Structural optimization system based on trabecular bone surface adaptation. *Struct. Multi. Optim.* **32**, 241–249 (2006)
55. Odgaard, A., Gundersen, H.J.G.: Quantification of connectivity in cancellous bone, with special emphasis on 3-D reconstructions. *Bone* **14**, 173–182 (1993)
56. Parfitt, A.M.: Implications of architecture for the pathogenesis and prevention of vertebral fracture. *Bone* **13**, S41–S47 (1992)
57. Podshivalov, L., Fischer, A., Bar-Yoseph, P.Z.: Multiresolution 2D geometric meshing for multiscale finite element analysis of bone micro-structures. *Virtual Phys. Prototyping* **5**, 33–43 (2010)
58. Podshivalov, L., Fischer, A., Bar-Yoseph, P.Z.: 3D hierarchical geometric modeling and multiscale FE analysis as a base for individualized medical diagnosis of bone structure. *Bone* **48**, 693–703 (2011)
59. Podshivalov, L., Holdstein, Y., Fischer, A., Bar-Yoseph, P.Z.: Towards a multi-scale computerized bone diagnostic system: 2D micro-scale finite element analysis. *Commun. Numer. Methods Eng.* **25**, 733–749 (2009)
60. Rho, J.-Y., Kuhn-Spearing, L., Zioupos, P.: Mechanical properties and the hierarchical structure of bone. *Med. Eng. Phys.* **20**, 92–102 (1998)
61. Rincón-Kohli, L., Zysset, P.: Multi-axial mechanical properties of human trabecular bone. *Biomech. Model. Mechanobiol.* **8**, 195–208 (2009)
62. Rubin, M.R., Dempster, D.W., Kohler, T., Stauber, M., Zhou, H., Shane, E., Nickolas, T., Stein, E., Sliney, J., Silverberg, S.J., Bilezikian, J.P., Müller, R.: Three dimensional cancellous bone structure in hypoparathyroidism. *Bone* **46**, 190–195 (2010)
63. Samet, H.: *The Design and Analysis of Spatial Data Structures*. Addison-Wesley, Reading, MA (1990)
64. Sheffer, A., Etzion, M., Rappoport, A., Bercovier, M.: Hexahedral mesh generation using the embedded voronoi graph. *Eng. Comput.* **15**, 248–262 (1999)
65. Tanck, E., Van Aken, J.B., Van der Linden, Y.M., Schreuder, H.W.B., Binkowski, M., Huizenga, H., Verdonchot, N.: Pathological fracture prediction in patients with metastatic lesions can be improved with quantitative computed tomography based computer models. *Bone* **45**, 777–783 (2009)

66. Ulrich, D., van Rietbergen, B., Weinans, H., R  gsegger, P.: Finite element analysis of trabecular bone structure: a comparison of image-based meshing techniques. *J. Biomech.* **31**, 1187–1192 (1998)
67. Van Lenthe, G.H., Voide, R., Boyd, S.K., Muller, R.: Tissue modulus calculated from beam theory is biased by bone size and geometry: implications for the use of three-point bending tests to determine bone tissue modulus. *Bone* **43**, 717–723 (2008)
68. Van Rietbergen, B.: Micro-FE analyses of bone: state of the art. In: Majumdar, S.B., Brian, K. (eds.) *Noninvasive Assessment of Trabecular Bone Architecture and the Competence of Bone*. Springer, Berlin/New York (2001)
69. Wehrli, F.W., Saha, P.K., Gomberg, B.R., Song, H.K., Snyder, P.J., Benito, M., Wright, A., Weening, R.: Role of magnetic resonance for assessing structure and function of trabecular bone. *Top. Magn. Reson. Imaging* **13**, 335–355 (2002)
70. Wehrli, F.W., Song, H.K., Saha, P.K., Wright, A.C.: Quantitative MRI for the assessment of bone structure and function. *NMR Biomed.* **19**, 731–764 (2006)
71. Weiner, S., Wagner, H.D.: The material bone: structure-mechanical function relations. *Annu. Rev. Mat. Sci.* **28**, 271–298 (1998)
72. Zaoui, A.: Continuum micromechanics: survey. *J. Eng. Mech.* **128**, 808–816 (2002)



<http://www.springer.com/978-3-642-24617-3>

Patient-Specific Modeling in Tomorrow's Medicine

Gefen, A. (Ed.)

2012, X, 534 p., Hardcover

ISBN: 978-3-642-24617-3